7-3-2014

Mineralogical Transformation and Electrochemical Nature of Magnesium-Rich Primers During Natural Weathering

Shashi S. Pathak
University of Southern Mississippi

Michael D. Blanton
University of Southern Mississippi

Sharathkumar K. Mendon
University of Southern Mississippi, sharathkumar.mendon@usm.edu

James W. Rawlins
University of Southern Mississippi, james.rawlins@usm.edu

Metals **2014**, *4*, 322-334; doi:10.3390/met4030322

OPEN ACCESS

metals

ISSN 2075-4701

www.mdpi.com/journal/metals/

Article

Mineralogical Transformation and Electrochemical Nature of Magnesium-Rich Primers during Natural Weathering

Shashi S. Pathak, Michael D. Blanton, Sharathkumar K. Mendon and James W. Rawlins *

School of Polymers and High Performance Materials, the University of Southern Mississippi, 118 College Drive #5217, Hattiesburg, MS 39406-0001, USA;
E-Mails: pathak.iitb@gmail.com (S.S.P.); michael.blanton@usm.edu (M.D.B.); sharathkumar.mendon@usm.edu (S.K.M.)

* Author to whom correspondence should be addressed; E-Mail: james.rawlins@usm.edu; Tel.: +1-601-266-5618; Fax: +1-601-266-5880.

Received: 15 May 2014; in revised form: 14 June 2014 / Accepted: 23 June 2014 / Published: 3 July 2014

Abstract: Magnesium-rich primers (MgRP) have generated great interest as a promising alternative to chromium-based primers for the protection of aluminum substrates but their performance during exterior exposure has not been well documented. This paper focuses on the evaluation of MgRP during natural weathering to gain insight into its mineralogical phase transformation and electrochemical nature. Control studies were conducted on Mg and AA2024-T3 coupons. The results indicate that Mg particles in MgRP transform into a variety of hydroxide, carbonate, and hydroxy carbonates. During natural weathering, CO_2 inhibited the dissolution of both Mg and AA2024-T3 as a result of protective carbonate layer formation in the coating.

Keywords: magnesium; corrosion; natural weathering

1. Introduction

Corrosion protection of aluminum alloys by Mg-rich primer (MgRP) is based on the principle of sacrificial cathodic polarization of aluminum by Mg. Mg (E^{Mg+2}/E^{Mg} = −1.6 V *vs.* SCE) is more active (*i.e.*, anodic) in the galvanic series than aluminum (E^{Al+3}/E^{Al} = −0.6 V *vs.* SCE) and AA2024-T3 alloying constituents. Mg can serve as a sacrificial anode by depressing the natural corrosion potential of aluminum to a value where it does not favor corrosion. MgRPs are considered an environmentally

responsible alternative to chromium-based primers for protecting aluminum structures. MgRPs contain sufficient Mg particles to maintain electrical contact with the aluminum substrate as well as each other. It is important to ensure that surface treatment, if any, on the aluminum does not create an electrical insulation between the Mg-rich primer and the aluminum substrate. Options to reduce the electrochemical activity of Mg in MgRP include the use of Mg alloys (with Al and Zn) [1] or forming a layer of Mg oxide/hydroxide/carbonate [2] at the expense of some reduction in the cathodic properties of pure Mg. Both these approaches decrease the galvanic protection offered by pure Mg.

MgRP stability is dependent on the nature of Mg particles (pure Mg, Mg alloy [1], Mg with oxide/hydroxide/carbonate layer [2] on it), coating matrix, insulating or non-insulating [3], and the environment to which it is exposed [4]. Panels coated with MgRPs have performed very well during outdoor exposure evaluation on test coupons at various sites across the US. However, concerns have been raised about premature blistering of MgRPs in aqueous and marine environments. It has also been observed that MgRPs fail rapidly and exhibit heavy blistering very early on in salt spray tests (ASTM B117), which is still a key test in certifying coatings for corrosion protection. In our previous work [4], we investigated the behavioral dichotomy of MgRP exposed to salt spray testing (ASTM B117) and natural weathering (in a non-marine, non-urban environment). The study revealed the presence of a thin and porous Mg hydroxide layer in primers exposed to salt spray, and a thicker, protective hydroxyl Mg carbonate (nesquehonite, $MgCO_3 \bullet 3H_2O$) layer in primers exposed to natural weathering. MgRPs exposed to dry atmospheric conditions exhibit excellent blistering resistance but marine conditions are inherently not conducive to Mg carbonate formation at a rate rapid enough to protect the primer against blistering.

Upon extended interaction with Mg, atmospheric concentration of CO_2 (~420 ppm) results in a protective layer of Mg carbonate or hydroxy carbonate. The effects of CO_2 interaction with Mg are dependent on CO_2 concentration, interaction time, and electrolyte nature (presence or absence of chloride). Lin *et al.* studied the role of CO_2 in the atmospheric corrosion of AZ91 Mg alloy in the presence of NaCl and concluded that CO_2 inhibited NaCl-induced corrosion by generating slightly soluble hydroxy carbonates that provided a partly protective layer on the surface of the Mg alloy [5]. Cathodic polarization studies on Mg-rich primer coated AA2024-T3 alloy [6] indicated that CO_2 in high concentrations buffers the pH on the AA2024-T3 surface and diminishes the extent of basic corrosion. It was also determined that the atmospheric concentration of CO_2 is not sufficient to prevent cathodic or basic corrosion. Mg particle dissolution results in basicity at the interface and is a primary requisite to cathodically protect aluminum from corrosion. Lindstrom *et al.* [7] reported that sodium chloride-induced atmospheric corrosion of Mg alloys (AM20, AM50, and AZ91) was inhibited by ambient concentrations of CO_2. Corrosion rates were about three times greater in the absence of CO_2 than in the presence of 350 ppm CO_2. The inhibitive effect of CO_2 was partly attributed to the formation of a slightly protective carbonate-containing film on the alloy surface. Blücher *et al.* [8] reported that the NaCl-induced atmospheric corrosion of aluminum alloy AA 1070 is 10–20 times faster in CO_2-free humid air compared to air containing ambient levels of CO_2. The corrosion inhibition by CO_2 was explained on the basis of the neutralization of surface electrolytes. In a subsequent paper, Blücher *et al.* attributed the passivating effect of CO_2 on the NaCl-induced corrosion of AZ91D to the $Mg_5(CO_3)_4(OH)_2 \bullet 5H_2O$ layer formed on the surface of AZ91D [9].

The inhibitive effect of CO_2 on Mg alloy AZ 31B was investigated via potentiodynamic polarization and electrochemical impedance measurements in NaCl solutions of different concentrations that were saturated with CO_2 [10]. The corrosion current decreased and the corrosion potential shifted to a positive direction with increasing immersion time. Passive behavior was detected after eight hours of immersion and the passive range increased with increasing immersion times. The surface products on AZ91 were identified as MgO, $Mg(OH)_2$ and $Mg_2(OH)_3Cl$ in NaCl solution, MgO, $Mg(OH)_2$ and $Mg_2(OH)_2CO_3$ in water saturated with CO_2 (without NaCl), and MgO, $Mg(OH)_2$, $Mg_2(OH)_2CO_3$ and $Mg_2(OH)_3Cl$ in NaCl solution saturated with CO_2. The corrosion rate increased with increasing NaCl concentration in the presence and absence of CO_2. The corrosion rate in NaCl solution saturated with CO_2 was found to be higher than that in NaCl solution purged with inert gas.

In this investigation, we sought to determine the mineralogical transformation occurring on Mg particles (in Mg-rich primer) during natural weathering, the cathodic nature of Mg-rich primer (treated *vs.* untreated), and the impact of atmospheric CO_2 on AA2024-T3 and the electrochemical nature of Mg.

2. Results and Discussion

2.1. Behavior of MgRP (MgPUnt) in Laboratory Environment

Figure 1a reveals the dichotomous behavior of Mg-rich (MgPUnt) primer (on AA2024-T3 substrate) in an accelerated corrosion test environment (ASTM B117) and natural weathering (at Hattiesburg, a non-marine, non-industrial environment). Panels exposed directly and without carbonic acid pretreatment to the salt fog environment exhibited blister formation within four hours of exposure. Mineralogical studies using Scanning electron microscopy (SEM)/Energy dispersive X-ray spectroscopy (EDS) and Fourier transform infrared (FTIR) spectroscopy indicated the formation of brucite ($Mg(OH)_2$, flower-like morphology) on panels placed in the salt fog and nesquehonite ($MgCO_3 \cdot 3H_2O$, needle-like crystals) on panels exposed to natural weathering.

Mg-rich (MgPUnt) primer was applied on metal panels (AA2024 T3, cold rolled steel R-36, aluminum Al-36, and phosphated cold rolled steel) as well as polymeric sheets (Noryl® GTX) and dried at ambient for seven days before being placed in the salt-spray chamber (ASTM B117) to distinguish the influence of the substrate on blistering. As expected, blister formation occurred rapidly on all substrates (Figure 1b). This supports our hypothesis that blister formation is due to the electrochemical instability (high electrochemical reactivity) of Mg powder in the highly humid and chloride ion-rich environment of the salt fog chamber.

2.2. Behavior of MgRP in Marine Exposure Site

Mg-rich (MgPUnt) primer coated AA2024-T3 panels were exposed at Daytona Beach, Florida (USA). Needle-like crystalline features, similar to nesquehonite crystals, were observed on the primed panels after seven days of ambient beachside exposure. This observation supports the fact that Mg particles in Mg-rich (MgPUnt) primer interact with atmospheric CO_2 to form Mg carbonate/hydroxy carbonate as seen in the laboratory specimens. Figure 2 is an overlay of the optical image and FTIR

signature of typical needle-like crystals of nesquehonite on MgPUnt surface (Figure 2a), Mg cube (Figure 2b), and in treated Mg powder. Peak assignments are presented in Table 1.

Figure 1. (**a**) Surface features of Mg-rich (MgPUnt) primer coated on AA2024-T3 panels and exposed to salt-spray test (ASTM B117) and natural weathering. (**b**) Blistering of Mg-rich (MgPUnt) primer coated on metal panels (AA2024-T3, R 36, Al 36, and phosphated CR steel), and Noryl GTX sheet on exposure to salt-spray test (ASTM B117) for two days.

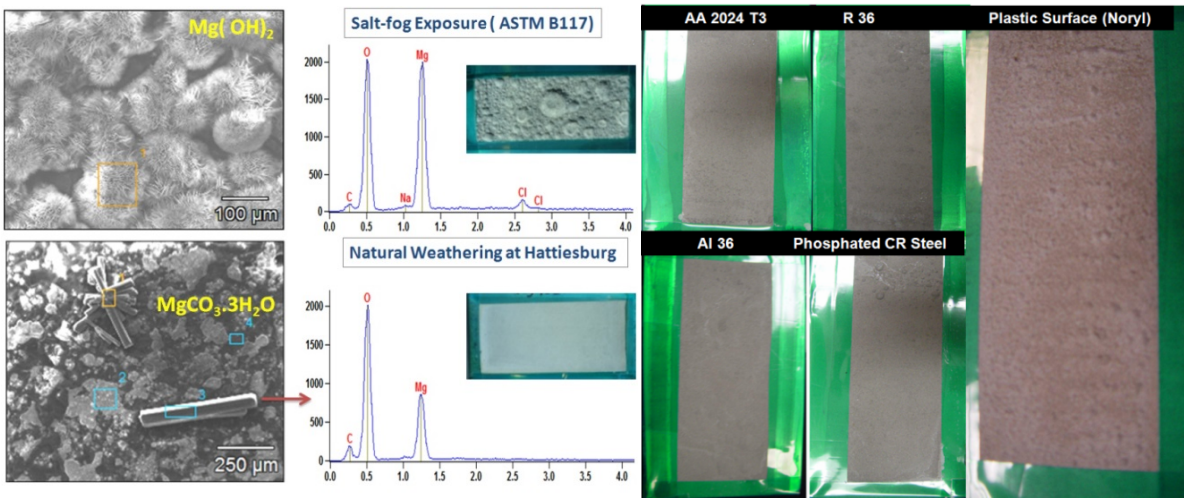

(**a**) (**b**)

Figure 2. Optical image and a Fourier transform infrared (FTIR) spectroscopy signature of needle-like crystals on Mg cube immersed in 3.5 wt% NaCl saturated with CO_2 (**a**) and MgPUnt primer exposed at Daytona beach for 30 days (**b**).

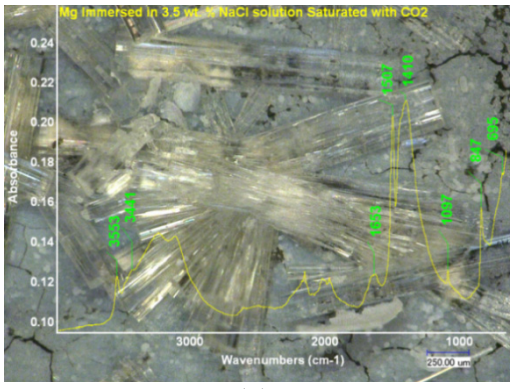

(**a**)

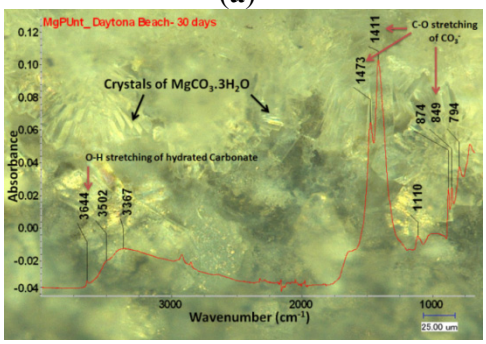

(**b**)

Table 1. Fourier transform infrared (FTIR) spectroscopy peak assignments.

Figure	Group/Chemical bond
2b	3652 cm^{-1} O–H stretching of $(OH)^-$ in hydromagnesite 3541 cm^{-1} O–H stretching of H_2O attached to hydrated Mg carbonate 1654 cm^{-1} O–H stretching of H_2O attached to hydrated Mg carbonate 1507 and 1408 cm^{-1} symmetric stretching mode of carbonate 846 cm^{-1} asymmetric stretching mode of carbonate 794 cm^{-1} from hydromagnesite
3a	2963, 2917 and 2872 cm^{-1} asymmetric and symmetric vibrations of the aliphatic $–CH_2–$ group of Eponol 3400 cm^{-1} O–H stretching of hydroxyl group of Eponol
3b	3700 cm^{-1} O–H stretching vibration in $Mg(OH)_2$ 3650 cm^{-1} $(OH)^-$ stretching of hydromagnesite 1418 cm^{-1} O–H stretching of H_2O attached to hydrated Mg carbonate
3c	3644 cm^{-1} $(OH)^-$ stretching of hydromagnesite 3502 cm^{-1} O–H stretching of H_2O attached to hydrated Mg carbonate 1473 and 1411cm^{-1} symmetric stretching mode of carbonate and 846 cm^{-1} asymmetric stretching mode of carbonate from hydromagnesite

Figure 3. FTIR spectra of MgPUnt coated AA2024-T3 at ambient (**a**), after exposure at Daytona beach for 7 days (**b**) and 30 days (**c**); and at the rain forest site and marine exposure in Hawaii (**d**).

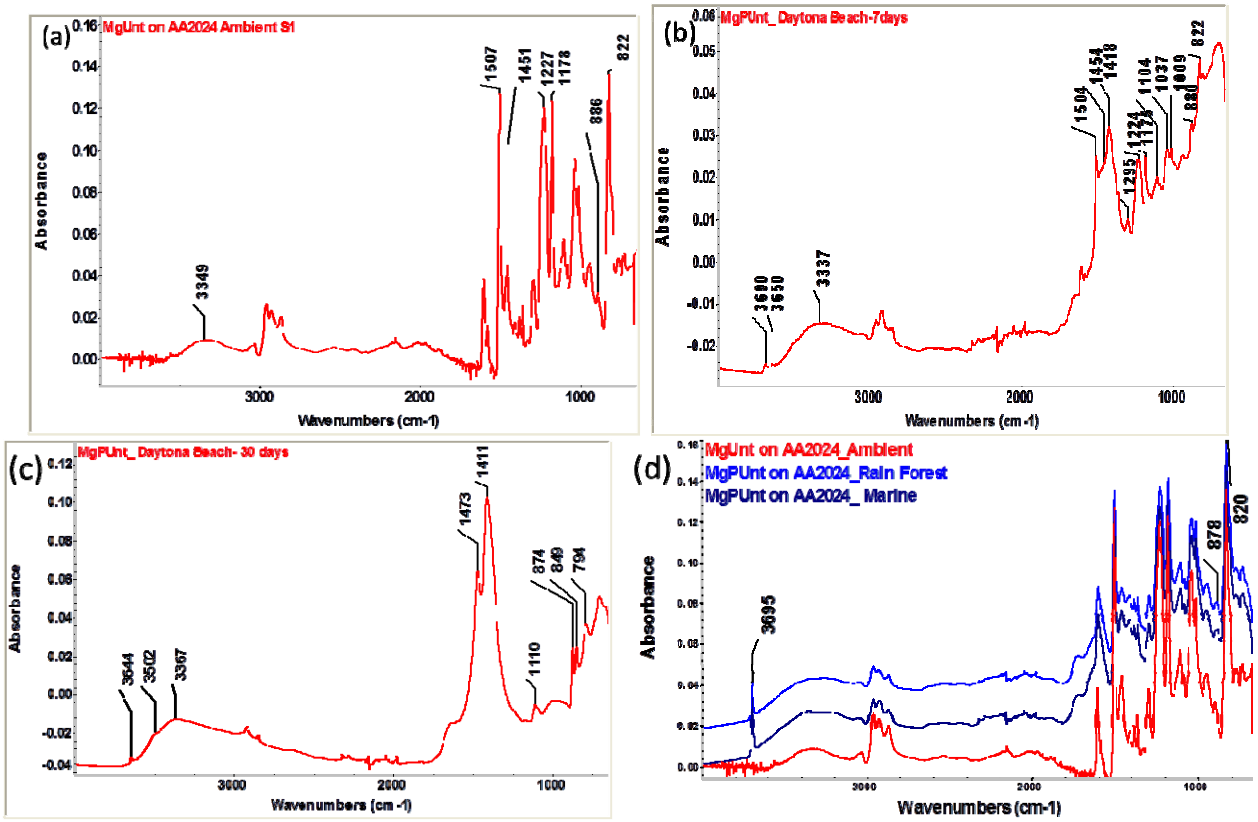

The FTIR signature (Figure 3) of the MgPUnt surface shows a sharp peak around 3690 cm^{-1} that is attributed to O–H stretching vibration of $Mg(OH)_2$, while the peaks around 3644 and 3502 cm^{-1} are due to stretching vibration bands of the magnesite (OH)− and H_2O, respectively. The band at 1643 cm^{-1} is identified as HCO_3^- stretching vibration, the sharp CO_3^{-2} stretching vibration peaks around 1473 and 1411 cm^{-1} arise from nesquehonite and hydromagnesite, the broader band around 1650 cm^{-1} is attributed to HCO_3^- stretching vibration, the band 1083 cm^{-1} is assigned to Mg–O stretching vibration of MgO, and the peak seen at 849 cm^{-1} is due to the CO_3^{-2} bending vibration band of nesquehonite and hydromagnesite.

The brucite peak (3690 cm^{-1}) was only observed on the panel that had been exposed at Daytona Beach for seven days. After 30 days exposure, the panel exhibited a new carbonate peak at 864 cm^{-1} that confirmed the progressive conversion of Mg to brucite, nesquehonite, and hydromagnesite. Coated MgPUnt panels exposed at the rain forest and marine sites in Hawaii for six months exhibited a brucite peak at 3695 cm^{-1}. However, no peaks were observed for carbonate formation (Figure 3d).

Figure 4 shows the X-ray diffraction (XRD) patterns of (a) bare AA2024-T3 and MgPUnt coated on AA2024-T3 and exposed at (b) Hawaii (marine exposure) and (c) Daytona beach (7 days and 30 days). XRD patterns (Figure 4b) of MgPUnt exposed at Hawaii confirm the presence of $Mg(OH)_2$ (brucite) and hydroxy Mg carbonate (nesquehonite). The panels exposed at Daytona exhibited the presence of brucite and nesquehonite. All the peaks in the XRD pattern of the MgPUnt are in good agreement with the peaks characteristic of hydroxy Mg carbonate (JCPDS 70-1177), Mg hydroxide (JCPDS 07-0239), and nesquehonite (JCPDS 70-1433).

Figure 4. X-ray patterns of bare AA2024-T3 and MgPUnt on AA2024-T3 (**a**), MgPUnt on AA2024-T3 exposed at Hawaii (marine exposure) (**b**), and MgPUnt exposed at Daytona beach. Florida (**c**). Phases identified: (○) $Mg(OH)_2$ (brucite); (☆) hydroxy Mg carbonate (nesquehonite); (□) Mg; and (Δ) AA2024-T3.

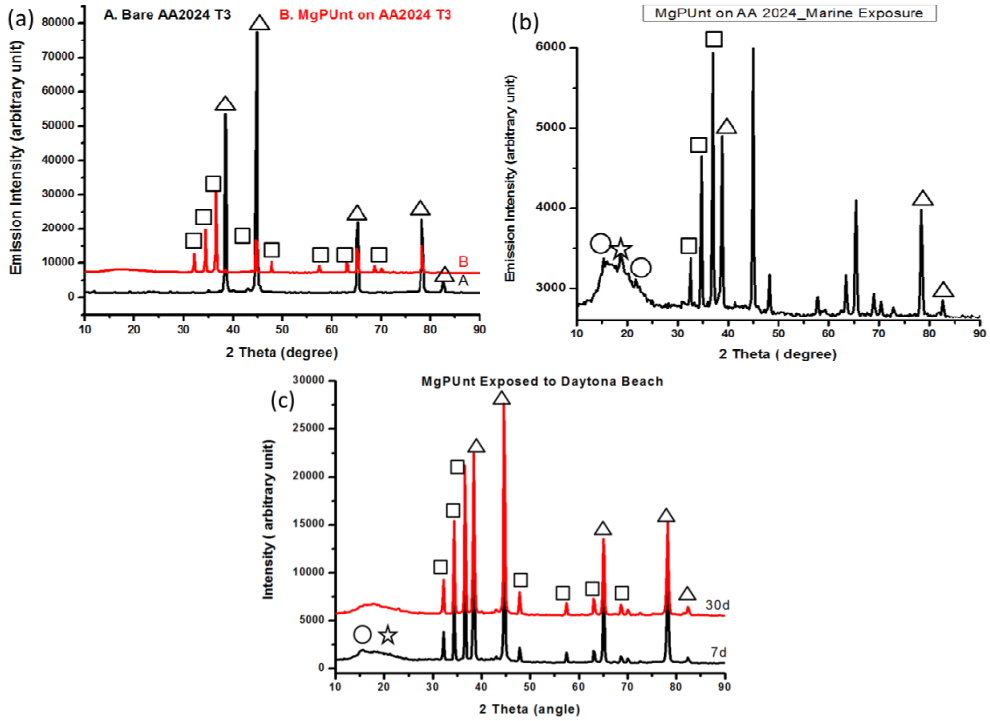

This observation supports our hypothesis that Mg particles interact with CO_2 even at atmospheric concentrations to form various carbonates and hydroxy carbonates. The extent and kinetics of Mg-CO_2 formation and interactions depends on the environmental severity, *i.e.*, humidity, level of salinity, CO_2 solubility, and presence of topcoat over Mg primer.

2.3. Electrochemical Response of MgRP (MgPUnt and MgPT)

The open circuit potentials (OCPs) of Mg cube, bare AA2024 T3, MgPUnt and MgPT were monitored for an hour in 3.5 wt% NaCl solutions to comprehend the galvanic coupling between the Mg particles in the coating and the AA2024-T3 substrate. The results are presented as an OCP *vs.* time plot in Figure 5. The OCP values of MgPUnt and MgPT show a mixed potential (*i.e.*, OCPMg cube <OCPMgPUnt and OCPMgPT <OCPAA2024-T3) and lie in between Mg and AA2024-T3. The OCP values of MgPUnt and MgPT stabilize at significantly greater negative potentials than that of AA2024-T3, indicating the cathodic nature of treated Mg-rich primers. The variations in OCP values of our MgRP are in good agreement with those reported in the literature on Mg-rich primers. Treated MgPT is always less cathodic than MgPUnt. The extent of Mg particle treatment is critical since extended treatment times will result in loss of the cathodic protection afforded by Mg.

Figure 5. Open circuit potential (OCP) values of Mg cube, bare AA2024 T3, MgPUnt and MgPT monitored for an hour in a 3.5 wt% NaCl solution.

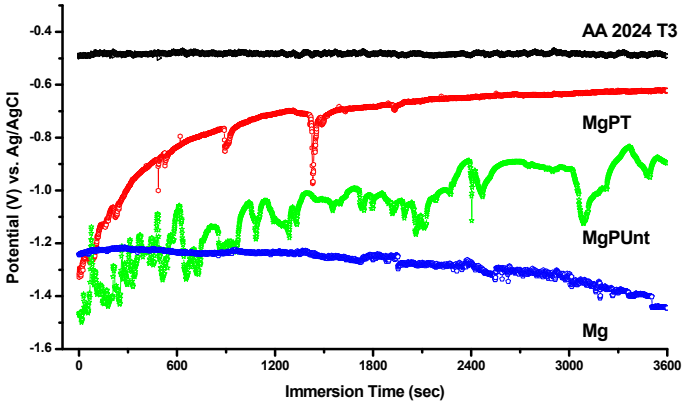

2.4. Impact of CO_2 on Electrochemical Response of MgPUnt

The effect of carbon dioxide on MgPUnt coated AA2024-T3 was characterized via polarization studies in 3.5 wt% NaCl solution with and without CO_2. The representative OCP and polarization curves for coated panels are shown in Figure 6. Panels immersed in NaCl solution saturated with CO_2 exhibited a novel OCP (Figure 6a) and lower corrosion current density (Figure 6b). The OCP of MgPUnt in NaCl solution saturated with CO_2 started at −100 mV and slowly dropped to stabilize around −900 mV. At ambient (atmospheric) levels of CO_2, MgPUnt coated panels exhibited a different trend in OCP, starting at −700 mV and increasing to −1.45 mV. The sharp decrease in potential after 900 seconds and 2500 seconds in the presence of saturated and ambient CO_2 levels, respectively, is likely to have been caused by the NaCl solution reaching the primer-metal interface and establishing a galvanic circuit between the AA2024-T3 substrate and the primer.

Figure 6. Potentiodynamic polarization curves (**a**) and OCP (**b**) of MgPUnt coated AA2024 panels in 3.5 wt% NaCl solution saturated with CO_2 and ambient level of CO_2.

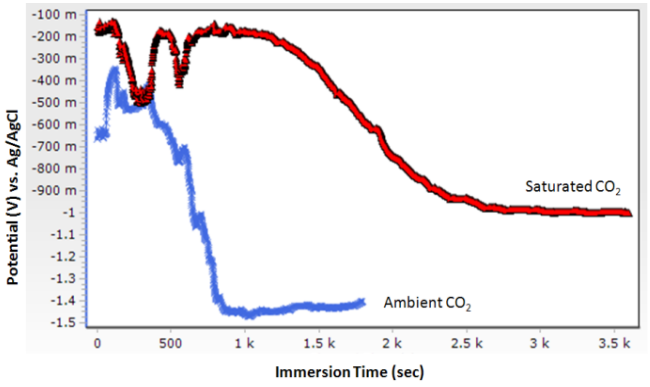

(**a**)

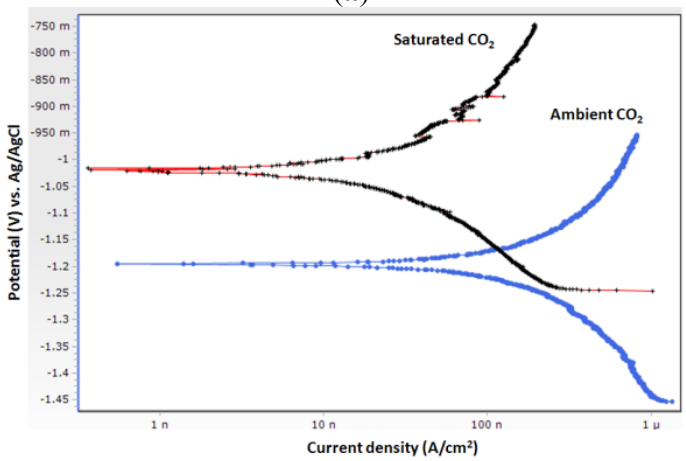

(**b**)

The OCP polarization plots show that the corrosion potential (Ecorr) of the panels in NaCl solution saturated with CO_2 moved to the positive direction by approximately 200 mV relative to the panel immersed in NaCl solution with ambient CO_2. The corrosion current density of the representative panel immersed in NaCl solution and saturated with CO_2 is far smaller than that of the panel immersed in NaCl solution with ambient CO_2. Both OCP and polarization experiments suggest that CO_2 shifts the coating towards a lower corrosion current density and corrosion potential and supports our other observations.

2.5. Impact of Pre-Immersion Time in NaCl-CO_2 Solution on Electrochemical Response of Mg

In air, Mg forms a gray layer of Mg oxide on its surface that converts to Mg hydroxide in the presence of moisture. Mg hydroxide is stable only at basic pH. On the other hand, CO_2 is acidic in nature. To better understand the role of CO_2 on the Mg-rich primer, the electrochemical response of Mg was determined in 3.5 wt% NaCl under the following exposure conditions:

(a) 3.5 wt% NaCl at ambient level of CO_2, no pre-immersion,
(b) 3.5 wt% NaCl saturated with CO_2, no pre-test immersion (before electrochemical testing),
(c) 3.5 wt% NaCl saturated with CO_2, 18 h pre-test immersion,
(d) 3.5 wt% NaCl saturated with CO_2, 6 days pre-test immersion, and
(e) 3.5 wt% NaCl at ambient level of CO_2, 24 h pre-test immersion.

CO_2 was bubbled through an aqueous solution of 3.5 wt% NaCl for 45 min to yield a saturated solution (pH value ~4.1). As expected, immersion of Mg coupons in this solution resulted in the formation of a gray layer on its surface. The effect of CO_2 on the electrochemical response of Mg in 3.5 wt% NaCl solution with saturated and ambient levels of CO_2 is presented in Figure 7. The OCP of Mg coupons moved towards a more noble direction with increasing immersion time in the presence of both ambient and saturated levels of CO_2. With increasing immersion time, the anodic branches shifted in the positive potential direction indicating that (a) the anodic dissolution was progressively retarded, and (b) the formation of a passive film on the Mg surface that reduces the corrosion current density has occurred.

Figure 7. Potentiodynamic polarization curves (**a**) and OCP (**b**) of Mg coupons in 3.5 wt % NaCl solution under various conditions: (A) 3.5 wt% NaCl at ambient levels of CO_2 , no pre-immersion (B) 3.5 wt% NaCl saturated with CO_2, no pre-test immersion (before electrochemical testing) (C) 3.5 wt% NaCl saturated with CO_2, 18 h pre-test immersion, (D) 3.5 wt% NaCl saturated with CO_2, 6 days pre-test immersion, and (E) 3.5 wt% NaCl saturated with CO_2, 24 h pre-test immersion.

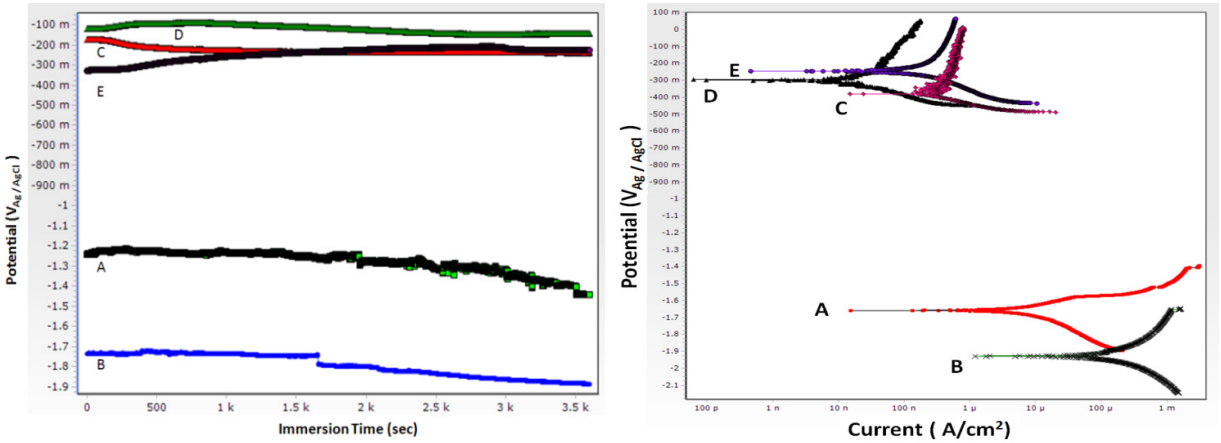

(**a**) (**b**)

OCP and polarization curves under conditions A, B, C, D, and E (Figure 7a) indicate that the pre-immersed samples exhibit lower corrosion current density and noble corrosion potential compared to samples without pre-immersion. Polarization plots of immersion under conditions A and E when compared to those of B, C and D suggest that even ambient levels of CO_2 can create a passive layer during the pre-test immersion which reduces the corrosion current density and moves the OCP towards a positive direction.

These observations are in good agreement with the observations reported by Qua *et al.* [10] on the corrosion behavior of AZ31B Mg alloy in NaCl solutions saturated with CO_2. The authors suggested that passivation of AZ31B in NaCl solutions saturated with CO_2 will occur if the immersion time is >8 h and the passive range increased with increasing immersion time. Longer immersion durations facilitate the formation of thick insoluble hydroxy Mg carbonates which restrict and/or limit electrolyte access to the cathodic Mg surface and improve the inhibitive properties.

2.6. Impact of CO_2 on Electrochemical Response of AA2024-T3

To understand the neutralizing effect of CO_2 on AA2024-T3 substrates, OCP and polarization experiments were performed on AA2024-T3 panels in 3.5 wt% NaCl solution with ambient and saturated levels of CO_2 (Figure 8). It was determined that CO_2 shifted the corrosion potential towards the cathodic direction as had been observed by Maier *et al.* [6] and reveals that the beneficial effect of CO_2 is not only limited to Mg but also extends to AA2024-T3 with minimal CO_2 exposure in advance of being introduced to a corrosive environment.

Figure 8. Potentiodynamic polarization curves (**a**) and OCP (**b**) of AA 2024-T3 coupons in 3.5 wt% NaCl solution.

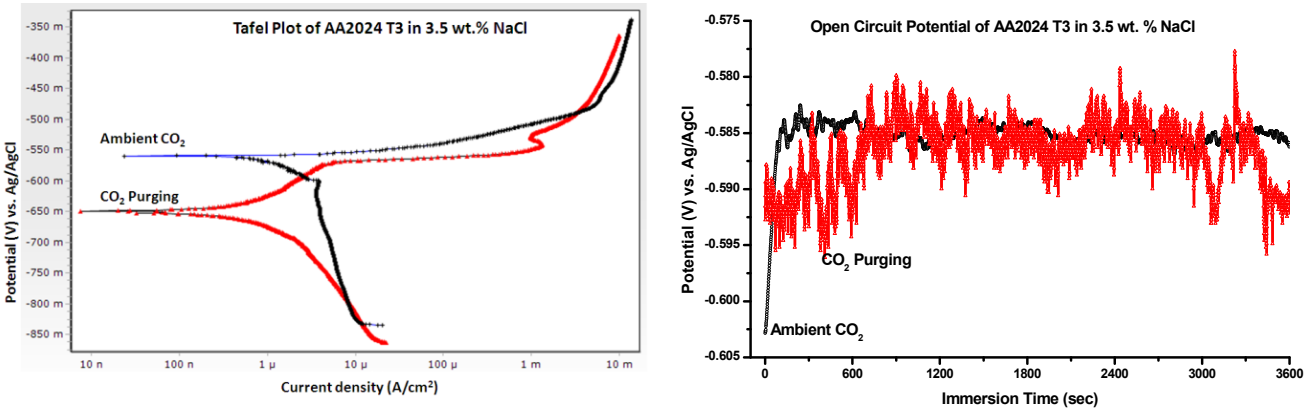

(**a**) (**b**)

However, the behavior of MgPUnt, Mg, or AA2024-T3 in a NaCl solution cannot be directly correlated to the system's behavior during atmospheric exposure. Compared to bulk NaCl solution, the surface electrolyte experiences insufficient convection in atmospheric conditions and the natural surface layer tends to remain where that layer is formed unless leached away by water. Moreover, since the diffusion paths for oxygen molecules are short, oxygen supply is usually not rate-limiting for the cathodic reaction. Blücher *et al.* [11] found that ambient level of CO_2 strongly inhibits the NaCl-induced atmospheric corrosion of Al in humid air by buffering the hydroxide formed at the cathodes and preventing the formation of aluminates.

3. Experimental Section

3.1. Materials

Mg cubes (19 mm × 19 mm × 6 mm) and Mg powder (325 mesh, 99.8% pure) were purchased from Alfa Aesar. Eponol® resin 53-BH-35 (Hexion Specialty Chemicals, Inc., Norco, CA, USA) is an ultra-high molecular weight bisphenol-A-based epoxy resin supplied as a 35% solution (by weight) in a blend of methyl ethyl ketone and propylene glycol methyl ether (75:25 by wt), and reported to have a specific gravity of 0.934 at 25 °C and 26.6% volume solids. CO_2 gas cylinders and sodium chloride were purchased from Nordan Smith (Hattiesburg, MS, USA) and Aldrich Chemicals (Milwaukee, WI, USA), respectively. All chemicals were used as received. Aerospace grade aluminum alloy AA2024-T3 was purchased from the Q-Panel Company (Westlake, OH, USA).

3.2. Treatment of Mg Powder in CO_2-H_2O

Mg particles were immersed for 30 min in an aqueous carbonic acid (saturated solution of CO_2-H_2O, pH 4.1 at ambient) solution to develop a layer of protective Mg carbonate [2]. The treated powder was used to formulate MgRP with Eponol. Mg cubes and AA2024-T3 coupons were also treated similarly in carbonic acid. Bare AA2024-T3 and Mg coupons (180 cm × 180 cm × 4 mm) were abraded with emery paper from 100–600 grit, cleaned with distilled water and acetone, and dried at ambient before use.

3.3. Preparation and Application of Mg-Rich Primer

MgRPs (with treated and untreated Mg powder) formulated at a pigment volume concentration (PVC) of 45% were prepared by blending Mg powder with Eponol overnight in a ball mill. The primers were applied on AA2024-T3 panels and Noryl GTX (a blend of polyphenylene oxide and polystyrene) plaques at 6 mils wet film thickness using an automated drawdown bar. The coated panels were kept in a dry box at ambient conditions for seven days prior to testing. The final dry film thickness was 75 ± 5 μm regardless of substrate type. The coated Al and Mg specimens were designated as: MgPT and MgPUnt (Mg-rich primer formulated with treated and untreated Mg particles, respectively), and MgT and MgUnt (Mg coupon treated and untreated).

3.4. Exposure Conditions

Coated AA2024-T3 panels were evaluated before and after exposure at marine and heavy rain forest sites in Daytona Beach, Florida and Hawaii, respectively. The electrochemical behavior of the coated AA2024-T3, AA2024-T3 substrate, and Mg coupons was investigated in an aqueous solution of 3.5 wt. % NaCl solution.

3.5. Characterization

The products on the surface of test specimens were characterized via Fourier transform infrared (FTIR) spectroscopy using a Digilab® FTS 2000 (Digilab, Inc., Marlborough, MA, USA). Spectra were collected in transmission mode over a frequency range of 600–4000 cm^{-1} via 256 scans at a resolution of 8 cm^{-1}. XRD is a non-destructive analytical technique that reveals information about the crystallographic structure, chemical composition, and physical properties of materials and thin films. XRD studies were conducted on a Rigaku Ultima3 X-ray diffractometer (Rigaku Americas Corporation, The Woodlands, TX, USA) at a scan speed of 0.5°/min and scan angles between $10° \leq 2\theta \leq 90°$.

Scanning electron microscopy (SEM) utilizes an electron beam for sample surface imaging at typical magnifications of 25–50,000×. Changes in the surface morphology of the primer, before and after exposure were examined on an FEI Quanta 200 (FEI, Hillsboro, OR, USA) equipped with a Thermo System 7 energy dispersive X-ray detector (Thermo Fisher Scientific, Inc., Waltham, MA, USA). Optical images of samples were collected using Keyence® VHX-600 digital microscopy system (Keyence Corporation of America, Itasca, IL, USA).

Electrochemical responses of the samples were evaluated by measuring their OCP, Tafel plot, and impedance values with potentiostat/galvanostat (VersaStatTM IV, Princeton Applied Research,

Oak Ridge, TN, USA) in a flat electrochemical cell (working electrode area 1 cm^2, cell capacity 250 cm^2, Model KO235 from Princeton Applied Research, USA). Test samples, platinum mesh, and Ag/AgCl saturated KCl served as working, counter, and reference electrodes, respectively. A Luggin capillary was positioned between the reference electrode and working electrode (test samples) surface to minimize ohmic potential drop. Each sample was immersed in the test solution for an hour before measurement until a steady state was reached. All measurements were conducted at ambient conditions in aqueous 3.5 wt% NaCl solution with and without CO_2 purging. OCPs of test samples were collected before performing Tafel and impedance measurements. Tafel plots were obtained at a scan rate of 0.1666 mV s^{-1} starting at 250 mV below the OCP up to 250 mV above OCP (OCP −250 mV to OCP +250 mV).

4. Conclusions

(1) Mg particles in MgRP readily transform into Mg hydroxide, nesquehonite, and hydroxy Mg carbonates during exposure in a marine environment within 30 days at varying ratios depending upon environmental severity, material handling, and the balance of varying Mg in advance of exposure to corrosive and humid environments.

(2) Both environmental and laboratory conditions shifts the OCP for Mg and the relative ratios of each protective and dissolvable materials towards the noble direction and decreases the corrosion current density after long exposure in NaCl solutions saturated with CO_2.

(3) Inhibitive effects of CO_2 were also observed with increasing immersion time, indicating that CO_2 reduces the electrochemical activity, the corrosion potential, and yet preserves the system's overall ability to protect substrates until an abundant but yet undetermined level of magnesium carbonate is formed.

(4) Ambient levels of CO_2 passivate Mg as well AA2024-T3 resulting in improved corrosion resistance for materials with Mg as the means of protecting AA2024-T3.

Acknowledgments

The authors gratefully acknowledge the financial support of Engineer Research and Development Center (ERDC) through funding by the Department of Defense (W9132T-09-2-0019) and collaborative efforts for Corrosion Prevention and Understanding via the University Corrosion Collaboration working group comprised of the University of Virginia, the University of Hawaii, the Ohio State University, the Air Force Academy, the University of Akron, and The University of Southern Mississippi.

Author Contributions

James W. Rawlins organized the funding for this research. Shashi S. Pathak designed the experiments, prepared the panels, and conducted the analytical and electrochemical studies. Michael D. Blanton conducted the SEM studies and organized panel exposures at the different locations. S. K. Mendon formulated the Mg-rich primer and edited the manuscript. All authors contributed to discussing and revising.

Conflicts of Interest

The authors declare no conflict of interest.

References

1. Xu, H.; Battocchi, D.; Tallman, D.E.; Bierwagen, G.P. Use of Magnesium Alloys as Pigments in Magnesium-Rich Primers for Protecting Aluminum Alloys. *Corrosion* **2009**, *65*, 318–325.
2. Pathak, S.S.; Blanton, M.D.; Mendon, S.K.; Rawlins, J.W. Behavior of Magnesium-Rich Primers on AA2024-T3. *Corros. Sci.* **2010**, *52*, 3782–3792.
3. Li, J.; He, J.; Chisholm, B.J.; Stafslien, M.; Battocchi, D.; Bierwagen, G.P. An investigation of the effects of polymer binder compositional variables on the corrosion control of aluminum alloys using magnesium-rich primers. *J. Coat. Technol. Res.* **2010**, *7*, 757–764.
4. Pathak, S.S.; Blanton, M.D.; Mendon, S.K.; Rawlins, J.W. Investigation on dual corrosion performance of magnesium-rich primer for aluminum alloys under salt spray test (ASTM B117) and natural exposure. *Corros. Sci.* **2010**, *52*, 1453–1463.
5. Lin, C.; Li, X. Role of CO_2 in the initial stage of atmospheric corrosion of AZ91 magnesium alloy in the presence of NaCl. *Rare Metals* **2006**, 25, 190–196.
6. Maier, B.; Frankel, G.S. Behavior of Magnesium-Rich Primers on AA2024-T3. *Corrosion* **2011**, *67*, 055001:1–055001:15.
7. Lindström, R.; Johansson, L.-G.; Svensson, J.-E. The influence of NaCl and CO_2 on the atmospheric corrosion of magnesium alloy AZ91. *Mater. Corros.* **2003**, *54*, 587–594.
8. Blücher, D.B.; Svensson, J.-E.; Johansson, L.G. The NaCl-Induced Atmospheric Corrosion of Aluminum: The Influence of Carbon Dioxide and Temperature. *J. Electrochem. Soc.* **2003**, *150*, B93–B98.
9. Blücher, D.B.; Svensson, J.-E.; Johansson, L.G.; Rohwerder, M.; Stratmann, M. Scanning Kelvin Probe Force Microscopy: A Useful Tool for Studying Atmospheric Corrosion of MgAl Alloys *in situ*. *J. Electrochem. Soc.* **2004**, *151*, B621–B626.
10. Qua, Q.; Ma, J.; Wang, L.; Li, L.; Bai, W.; Ding, Z. Corrosion behaviour of AZ31B magnesium alloy in NaCl solutions saturated with CO_2. *Corros. Sci.* **2011**, *53*, 1186–1193.
11. Blücher, D.B.; Lindstrom, R.; Svensson, J.-E.; Johansson, L.G. The Effect of CO_2 on the NaCl-Induced Atmospheric Corrosion of Aluminum. *J. Electrochem. Soc.***2001**, *148*, B127–B131.